A $\mu_{1,1}$- or $\mu_{1,3}$-carboxylate bridge makes the difference in the magnetic properties of dinuclear Mn^{II} compounds†

Verónica Gómez,*[a] Montserrat Corbella,[a] Mercé Font-Bardia[b] and Teresa Calvet[b]

Received 23rd July 2010, Accepted 22nd September 2010
DOI: 10.1039/c0dt00902d

Six new dinuclear Mn^{II} compounds with carboxylate bridges have been synthesized and characterized by X-ray diffraction: $[\{Mn(phen)_2\}_2(\mu\text{-}RC_6H_4COO)_2](ClO_4)_2$ with R = 2-Cl (**1**), 2-CH_3 (**2**), 3-Cl (**3**), 3-CH_3 (**4**), 4-Cl (**5**) and 4-CH_3 (**6**). Compounds **1** and **2** show two $\mu_{1,3}$-carboxylate bridges in a *syn–anti* mode while compounds **3–6** present a very uncommon coordination mode of the carboxylate ligand: the $\mu_{1,1}$-bridge. The magnetic properties of these compounds are very sensitive to the bridging mode of the carboxylate ligands. While compounds **1** and **2** ($\mu_{1,3}$-bridge) display antiferromagnetic interactions, with J values of −1.41 and −1.66 cm^{-1}, respectively, compounds **3–6** ($\mu_{1,1}$-bridge) show ferromagnetic interactions, with J values of 1.01, 0.98, 1.04 and 1.06 cm^{-1}, respectively. It is worth noting that compounds **3–6** are the first of their class to be magnetically characterized. The EPR spectra at 4 K for compounds with antiferromagnetic coupling (**1** and **2**) are more complex than those for compounds with a ferromagnetic interaction (**3–6**). Quite good simulations can be obtained with the ZFS parameters of the Mn^{II} ion $D_{Mn} \sim 0.095$ cm^{-1} and $E_{Mn} \sim 0.025$ cm^{-1} for compounds **1** and **2** and $D_{Mn} \sim 0.060$ cm^{-1} and $E_{Mn} \sim 0.004$ cm^{-1} for compounds **3–6**.

Introduction

Manganese-based coordination compounds are of great interest not only due to their magnetic properties[1] but also because of their importance in bioinorganic chemistry, as many manganese compounds are being synthesized to mimic several metalloproteins such as catalase[2] and the oxygen-evolving complex (OEC) of photosystem II.[3]

Carboxylate ligands are excellent groups due to their biological relevance and their wide variety of coordination modes, such as monodentate terminal, chelating, bidentate bridging and monodentate bridging modes. There are diverse dinuclear Mn^{II} complexes reported in the literature showing only carboxylate bridges, whether one,[4] two,[5] three[6] or even four,[7] as well as other bridging ligands besides carboxylate ligands, like aquo, hydroxo or phenoxo/alkoxo.

Regarding dinuclear Mn^{II} compounds with just two carboxylate bridges, the most common coordination mode is the *syn–anti* $\mu_{1,3}$-bridging mode (Fig. 1). Although the number of this type of compound is relatively large,[8–10] not many of them are magnetically characterized[10] and there are even fewer with their EPR spectrum reported.[9k,10d,e]

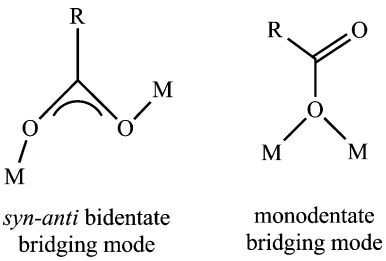

Fig. 1 Carboxylate binding modes involved in the compounds reported here.

Dinuclear Mn^{II} compounds displaying two carboxylate ligands in a monodentate bridging mode ($\mu_{1,1}$) (Fig. 1) are very rare. To our knowledge, there are very few complexes,[11–13] and in most of them the carboxylate groups form part of polydentate ligands.[11,12] However, this binding mode can be found in some 1D Mn^{II} systems.[14] Nevertheless, there are very few compounds with their magnetic properties studied[12,14c–e] or characterized by EPR spectroscopy.[13b,c]

In this paper, we report the synthesis of six new dinuclear Mn^{II} compounds with two carboxylate bridges with formula $[\{Mn(phen)_2\}_2(\mu\text{-}RC_6H_4COO)_2](ClO_4)_2$ with R = 2-Cl (**1**), 2-CH_3 (**2**), 3-Cl (**3**), 3-CH_3 (**4**), 4-Cl (**5**) and 4-CH_3 (**6**). All compounds (**1–6**) have been structurally characterized by X-ray diffraction and magnetically studied, leading to surprising results.

Experimental

Synthesis

All manipulations were carried out at room temperature under aerobic conditions. Reagents and solvents were obtained from commercial sources and used without further purification. The $Mn(n\text{-}RC_6H_4COO)_2 \cdot mH_2O$ (n = 2, 3, 4 and R = Cl, CH_3) were synthesized by the reaction of $MnCO_3$ and n-RC_6H_4COOH in

[a]*Departament de Química Inorgànica, Facultat de Química, Universitat de Barcelona, Martí i Franquès 1-11, 08028, Barcelona, Spain. E-mail: veronica.gomez@qi.ub.es; Fax: +34934907725; Tel: +34934039144*
[b]*Cristal.lografia, Mineralogia i Dipòsits Minerals, Universitat de Barcelona, Martí i Franquès s/n, 08028, Barcelona, Spain*

† Electronic supplementary information (ESI) available: Fig S1 View of π-stacking and C–H···π interactions between dinuclear units present in compound **2**. Fig. S2 View of π-stacking and C–H···C–H interactions between dinuclear units present in compound **4**. Fig. S3 View of interactions between perchlorate anions and dinuclear units present in compound **6**. Fig. S4 $Mn–O_b–Mn$ angle *vs.* Mn···Mn distance plot for compounds with $[Mn_2(\mu\text{-}O)_2]$ core. Fig. S5 Plot of $Mn–O_b$ *vs.* Mn···Mn distances for compounds with $[Mn_2(\mu\text{-}O)_2]$ core. CCDC reference numbers 785947–785952. For ESI and crystallographic data in CIF or other electronic format see DOI: 10.1039/c0dt00902d

boiling water. After several hours, the solution was filtered and concentrated, giving a pale pink precipitate of the desired product. Yields were calculated from the stoichiometric reaction.

[{Mn(phen)$_2$}$_2$(μ-2-ClC$_6$H$_4$COO)$_2$](ClO$_4$)$_2$ (1). Mn(2-ClC$_6$H$_4$COO)$_2$·2H$_2$O (0.60 g, 1.50 mmol), NaClO$_4$·H$_2$O (0.21 g, 1.50 mmol) and 1,10-phenanthroline (0.59 g, 3.00 mmol), all dissolved in absolute ethanol, were mixed (total volume ~ 75 mL) and stirred for 15 min. The yellow solid formed was isolated by filtration and dried in air. Yield 0.90 g, 88%. Anal. Calcd. for C$_{62}$H$_{40}$Cl$_4$Mn$_2$N$_8$O$_{12}$·H$_2$O (1358.73) (%): C, 54.80; H, 3.12; Cl, 10.44; N, 8.25. Found: C, 54.7; H, 3.1; Cl, 10.4; N, 8.0. Yellow crystals suitable for X-ray diffraction were obtained after several days by slow evaporation, in the refrigerator, of a solution of the dinuclear compound in 15 mL CH$_3$CN and a drop of water. Selected IR data (KBr pellet, cm^{-1}): 3417 (m), 3068 (w), 1601 (vs), 1516 (s), 1426 (s), 1401 (s), 1144 (m), 1089 (vs), 1050 (w), 864 (w), 845 (m), 759 (w), 725 (m), 638 (w), 623 (m).

[{Mn(phen)$_2$}$_2$(μ-2-CH$_3$C$_6$H$_4$COO)$_2$](ClO$_4$)$_2$ (2). The same procedure for the preparation of **1** was followed, using Mn(2-CH$_3$C$_6$H$_4$COO)$_2$·2H$_2$O (0.54 g, 1.50 mmol) in this case. The yellow solid formed was isolated by filtration and dried in air. Yield 0.76 g, 78%. Anal. Calcd. for C$_{64}$H$_{46}$Cl$_2$Mn$_2$N$_8$O$_{12}$ (1299.88) (%): C, 59.14; H, 3.57; Cl,5.45; N, 8.65. Found: C, 59.2; H, 3.6; Cl, 5.4; N, 8.7. Yellow crystals suitable for X-ray diffraction were obtained after several days by slow evaporation of the ethanolic mother liquor in the refrigerator. Selected IR data (KBr pellet, cm^{-1}): 3434 (m), 3067 (w), 2923 (w), 1623 (w), 1604 (m), 1583 (s), 1560 (s), 1516 (m), 1425 (s), 1403 (w), 1144 (w), 1120 (s), 1104 (vs), 864 (w), 848 (m), 751 (w), 728 (m), 637 (w), 623 (m).

[{Mn(phen)$_2$}$_2$(μ-3-ClC$_6$H$_4$COO)$_2$](ClO$_4$)$_2$ (3). An analogous procedure for the preparation of **1** was followed, using Mn(3-ClC$_6$H$_4$COO)$_2$·2H$_2$O (0.60 g, 1.50 mmol) in this case. A yellow solid was formed, isolated by filtration and dried in air. Yield 0.88 g, 88%. Anal. Calcd. for C$_{62}$H$_{40}$Cl$_4$Mn$_2$N$_8$O$_{12}$ (1340.71) (%): C, 55.54; H, 3.00; Cl, 10.58; N, 8.36. Found: C, 55.4; H, 3.0; Cl, 10.5; N, 8.2. Yellow crystals suitable for X-ray diffraction were obtained after several days by slow evaporation of a CH$_3$CN solution of compound **3** with a drop of water in the refrigerator. Selected IR data (KBr pellet, cm^{-1}): 3444 (m), 3061 (w), 1616 (s), 1592 (m), 1566 (m), 1519 (m), 1427 (s), 1310 (vs), 1260 (m), 1147 (m), 1085 (vs), 866 (m), 852 (vs), 779 (w), 766 (m), 730 (s), 640 (w), 623 (s).

[{Mn(phen)$_2$}$_2$(μ-3-CH$_3$C$_6$H$_4$COO)$_2$](ClO$_4$)$_2$ (4). The same procedure was followed as for compound **2**, using Mn(3-CH$_3$C$_6$H$_4$COO)$_2$·2H$_2$O (0.54 g, 1.50 mmol) in this case. A yellow solid was formed, isolated by filtration and dried in air. Yield 0.75 g, 77%. Anal. Calcd. for C$_{64}$H$_{46}$Cl$_2$Mn$_2$N$_8$O$_{12}$ (1299.87) (%): C, 59.14; H, 3.57; Cl, 5.45; N, 8.62. Found: C, 59.2; H, 3.6; Cl, 5.3; N, 8.4. Yellow crystals suitable for X-ray diffraction were obtained by mixing a CH$_3$CN solution of compound **4** with CH$_2$Cl$_2$ and layering this mixture with hexanes. Selected IR data (KBr pellet, cm^{-1}): 3416 (s), 3062 (w), 1616 (s), 1599 (m), 1580 (m), 1518 (m), 1427 (s), 1391 (w), 1314 (m), 1282 (w), 1213 (w), 1146 (w), 1097 (vs), 865 (w), 852 (m), 778 (w), 761 (m), 730 (s), 623 (m).

[{Mn(phen)$_2$}$_2$(μ-4-ClC$_6$H$_4$COO)$_2$](ClO$_4$)$_2$ (5). An analogous procedure was followed as for **1**, using Mn(4-ClC$_6$H$_4$COO)$_2$·2H$_2$O (0.60 g, 1.50 mmol) in this case. A yellow solid was formed, isolated by filtration and dried in air. Yield 0.87 g, 84%. Anal. Calcd. for C$_{62}$H$_{40}$Cl$_4$Mn$_2$N$_8$O$_{12}$·CH$_3$CH$_2$OH (1386.78) (%): C, 55.43; H, 3.34; Cl, 10.23; N, 8.08. Found: C, 55.5; H, 3.1; Cl, 10.0; N, 8.1. Yellow crystals suitable for X-ray diffraction were obtained by mixing a CH$_3$CN solution of compound **5** with CH$_2$Cl$_2$ and layering this mixture with hexanes. Selected IR data (KBr pellet, cm^{-1}): 3444 (m), 3083 (w), 3057 (w), 1609 (s), 1592 (m), 1567 (w), 1519 (w), 1429 (s), 1302 (s), 1145 (w), 1090 (vs), 865 (w), 850 (s), 782 (m), 729(s), 623 (m).

[{Mn(phen)$_2$}$_2$(μ-4-CH$_3$C$_6$H$_4$COO)$_2$](ClO$_4$)$_2$ (6). The same procedure for the preparation of **2** was followed, using Mn(4-CH$_3$C$_6$H$_4$COO)$_2$·2H$_2$O (0.54 g, 1.50 mmol) in this case. The pale yellow solid formed was isolated by filtration and dried in air. Yield 0.80 g, 82%. Anal. Calcd. for C$_{64}$H$_{46}$Cl$_2$Mn$_2$N$_8$O$_{12}$ (1299.87) (%): C, 59.14; H, 3.57; Cl, 5.45; N, 8.62. Found: C, 59.1; H, 3.6; Cl, 5.3; N, 8.6. Yellow needle-like crystals suitable for X-ray diffraction were obtained by mixing a CH$_3$CN solution of compound **6** with CH$_2$Cl$_2$ and layering this mixture with hexanes. Selected IR data (KBr pellet, cm^{-1}): 3442 (s), 3081 (w), 3056 (w), 1623 (m), 1606 (vs), 1570 (m), 1519 (m), 1430 (s), 1367 (w), 1308 (vs), 1295 (vs), 1224 (w), 1211 (w), 1176 (w), 1145 (m), 1099 (vs), 1018 (w), 963 (w), 865 (m), 854 (s), 775 (s), 730 (vs), 723 (s), 639 (w), 623 (m), 611 (w).

Physical measurements

Analyses of C, H, N and Cl were carried out by the "Servei de Microanàlisi" of the "Consell Superior d'Investigacions Científiques (CSIC)". Infrared spectra were recorded on KBr pellets, in the range 4000–400 cm^{-1}, with a Thermo Nicolet Avatar 330 FT - IR spectrometer. Magnetic susceptibility measurements between 2 and 300 K were carried out in a Quantum Design MPMP SQUID Magnetometer at the "Unitat de Mesures Magnètiques (Universitat de Barcelona)". Two different magnetic fields were used for the susceptibility measurements, ~ 200 G (2–5 K) and 3000 G (2–300 K), with superimposable graphs. Pascal's constants were used to estimate the diamagnetic corrections for the compound. The fit was performed by minimising the function $R = \Sigma [(\chi_M T)_{exp} - (\chi_M T)_{calc}]^2 / \Sigma (\chi_M T)_{exp}]^2$. Solid-state EPR spectra were recorded at X-band (9.4 GHz) frequency using a Bruker ESP-300E spectrometer, from room temperature to 4 K at the "Unitat de Mesures Magnètiques (Universitat de Barcelona)". The computational package easyspin[15] was used to simulate the solid-state EPR spectra of dinuclear compounds, considering all the spin states and including the magnetic interaction between the Mn^{II} ions (J) and the zero-field splitting parameters for each manganese ion (D_{Mn} and E_{Mn}) in the calculations.

X-ray diffraction data collection and refinement

X-ray diffraction measurements and resolution of compounds **1**–**5** were carried out at the "Unidade de Raios X (Universidade de Santiago de Compostela)" while compound **6** was elucidated at the "Unitat de Difracció de Raigs X (Serveis Cientificotècnics, Universitat de Barcelona)". Crystals of compounds **1**–**5**, obtained as described in the experimental section, were mounted onto a sealed tube and X-ray crystallographic data were collected at 100 K. All measurements were made on a Bruker Apex-II CCD diffractometer with graphite monochromated Mo-Kα radiation (λ = 0.7107 Å). The structures were solved using the

Table 1 Crystallographic data for compounds **1–6**

	1·6CH_3CN	**2**·2CH_3CH_2OH	**3**	**4**	**5**	**6**
Chemical formula	$C_{74}H_{58}Cl_4Mn_2N_{14}O_{12}$	$C_{68}H_{58}Cl_2Mn_2N_8O_{14}$	$C_{62}H_{40}Cl_4Mn_2N_8O_{12}$	$C_{64}H_{46}Cl_2Mn_2N_8O_{12}$	$C_{62}H_{40}Cl_4Mn_2N_8O_{12}$	$C_{64}H_{46}Cl_2Mn_2N_8O_{12}$
Formula weight	1587.02	1392.00	1340.70	1299.87	1340.70	1299.87
Crystal colour, habit	yellow, prism	yellow, prism	yellow, prism	colourless, prism	colourless, prism	yellow, prism
T/K	100(2)	100(2)	100(2)	100(2)	100(2)	248(2)
λ (Mo-Kα)/Å	0.7107	0.7107	0.7107	0.7107	0.7107	0.7107
Crystal system	triclinic	triclinic	triclinic	triclinic	monoclinic	monoclinic
Space group	$P\bar{1}$	$P\bar{1}$	$P\bar{1}$	$P\bar{1}$	$C2/m$	$C2/m$
Crystal size/mm	0.44 × 0.29 × 0.14	0.46 × 0.32 × 0.18	0.34 × 0.30 × 0.05	0.33 × 0.17 × 0.17	0.18 × 0.09 × 0.09	0.2 × 0.1 × 0.1
a/Å	12.6230(6)	9.4995(3)	9.5307(2)	9.5435(4)	14.585(2)	14.975(8)
b/Å	13.0026(3)	13.1136(4)	12.0676(2)	12.0805(5)	19.584(3)	20.112(6)
c/Å	13.3200(4)	14.1160(4)	13.4362(3)	13.3549(5)	9.5953(13)	9.582(5)
α /°	116.6890(10)	111.089(2)	65.6420(10)	66.425(2)	90	90
β /°	106.457(2)	95.032(2)	88.2400(10)	88.325(2)	96.055(9)	96.48(3)
γ /°	94.124(2)	102.951(2)	84.0110(10)	84.093(2)	90	90
V/Å^3	1821.98(10)	1571.31(9)	1399.96(5)	1403.57(10)	2725.4(7)	2867(2)
Z	1	1	1	1	2	2
ρ_c/g cm^{-3}	1.446	1.471	1.590	1.538	1.634	1.506
μ/mm^{-1}	0.57	0.56	0.72	0.62	0.74	0.61
F(000)	814	718	682	666	1364	1332
θ range/°	2.4 to 26.4	2.7 to 24.4	2.7 to 30.5	2.7 to 25.8	2.6 to 25.5	2.6 to 32.3
Index ranges	h = −15 → 14 k = −16 → 14 l = 0 → 16	h = −11 → 11 k = −15 → 14 l = 0 → 17	h = −13 → 13 k = −15 → 17 l = 0 → 19	h = −11 → 11 k = −15 → 15 l = −16 → 16	h = = −18 → 18 k = 0 → 24 l = 0 → 11	h = −22 → 22 k = −30 → 30 l = −12 → 13
Data/restraints/parameters	7427/0/481	5947/4/436	8521/0/455	5596/189/462	2878/0/237	4730/2/233
Goodness-of-fit on F^2	1.01	1.09	1.05	1.05	1.28	1.10
R_1[a], wR_2[b] [$I > 2\sigma(I)$]	0.0352, 0.0971	0.033, 0.0788	0.0336, 0.086	0.0374, 0.0838	0.086, 0.2048	0.0625, 0.1512
R_1[a], wR_2[b] (all data)	0.0468, 0.1004	0.0396, 0.0817	0.0437, 0.091	0.0588, 0.0920	0.1063, 0.2106	0.1129, 0.1709

[a] $R_1 = \sum\|F_o| - |Fc\|/\sum|F_o|$. [b] $wR_2 = \{\sum[w(F_o^2 - F_c^2)^2]/\sum[w(F_o^2)^2]\}^{1/2}$, $w = 1/[\sigma^2(F_o^2) + (aP)^2 + bP]$, where $P = [\max(F_o^2,0) + 2F_c^2]/3$.

SIR97 program[16] and refined by full-matrix least-squares method using the SHELXL97 program.[17] Hydrogen atoms were treated by a mixture of independent and constrained refinement. A crystal of compound **6**, obtained as described in the experimental section, was mounted on a MAR345 diffractometer with an image plate detector and graphite monochromated Mo-Kα radiation (λ = 0.7107 Å). The structure was solved using the SHELXS program[18] and refined by a full-matrix least-squares method with the SHELX97 program.[17] Hydrogen atoms were computed and refined using a riding model with an isotropic temperature factor equal to 1.2 times the equivalent temperature factor of the atom which is linked. Crystal data collection and refinement parameters for all compounds (**1–6**) are given in Table 1.

Results and discussion

Synthesis

In previous papers we reported that the reaction between manganese(II) carboxylates and bidentate nitrogenated ligands (NN) leads to different types of compounds depending on the Mn^{II}/NN ratio and the presence or absence of ClO_4^-.[10d,e,19] In the present work, we carried out the reaction between $Mn(RC_6H_4COO)_2{\cdot}mH_2O$ (R = 2-Cl, 2-CH_3, 3-Cl, 3-CH_3, 4-Cl, 4-CH_3), 1,10-phenanthroline (phen) and $NaClO_4$ in a 1 : 2 : 1 ratio, obtaining ionic dinuclear compounds with formula $[\{Mn(phen)_2\}_2(\mu\text{-}RC_6H_4COO)_2](ClO_4)_2$ (**1–6**) in all cases. However, although the procedure followed to synthesize these dinuclear compounds was the same, two different modes of coordination of the carboxylate ligand are found. Compounds with the R substituent in the *ortho* position show a $\mu_{1,3}$-coordination mode while compounds with R in the *meta* or *para* position show a $\mu_{1,1}$-coordination mode. This different coordination mode of the carboxylate ligand can be observed in the IR spectra. These compounds show different bands in the range 1620–1300 cm^{-1} due to the carboxylate groups. For compounds **1** and **2**, two strong bands at ~ 1603 and ~ 1403 cm^{-1} can be assigned to the asymmetric and symmetric vibrations from the carboxylate groups, with values of $\Delta = \nu_a(COO) - \nu_s(COO)$ of ~ 200 cm^{-1}, which are indicative of carboxylate ligands coordinated in a bidentante bridging mode ($\mu_{1,3}$).[20] However, the IR spectra of compounds **3–6** show these two strong bands at ~ 1612 and ~ 1309 cm^{-1}, with a Δ value of ~ 303 cm^{-1}, indicating that the carboxylate ligands are bridged in a monatomic mode ($\mu_{1,1}$).[20] On the other hand, broad bands at ~ 1100 cm^{-1} and a moderate intensity band at 623 cm^{-1} are assigned to the perchlorate ions. The phen ligand shows characteristic bands at 1518, 1427, 865, 850 and 723 cm^{-1}.

The formation of the dinuclear complex could be explained by the assembly of two mononuclear fragments, both with a monodentate carboxylate. This assembly can be through the O_2 atom, leading to a $\mu_{1,3}$-bridging mode, or through the O_1 atom, which leads to a $\mu_{1,1}$-bridge (Scheme 1). Two factors can contribute to this different behavior: the steric and the electronic effects. The electronic effect of the R group (Me or Cl) is very different, however the coordination mode of the carboxylate depends on the position of the substituent (*ortho* or *meta* and *para*) in the phenyl ring. So, the steric effect appears to be the most important factor in the type of bridge formed in the dinuclear complex. Moreover, it is interesting to note that analogous compounds to **1**, **3** and **5** with 2,2′-bipyridine (bpy) instead of phen show a $\mu_{1,3}$ coordination

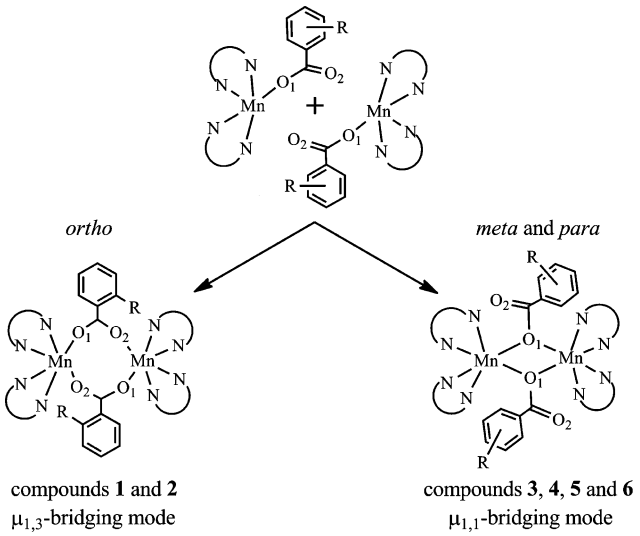

Scheme 1 The two coordination modes of the carboxylate bridge found for compounds reported here.

mode (deducible from their IR spectra),[9j,10e] so the phen ligand also seems to play an important role in the different behavior observed.

Description of structures

[{Mn(phen)$_2$}$_2$(μ-2-ClC$_6$H$_4$COO)$_2$](ClO$_4$)$_2$·6CH$_3$CN (1·6CH$_3$CN) and [{Mn(phen)$_2$}$_2$(μ-2-CH$_3$C$_6$H$_4$COO)$_2$](ClO$_4$)$_2$·2CH$_3$CH$_2$OH (2·2CH$_3$CH$_2$OH). The cationic structures of compounds **1** and **2** are depicted in Fig. 2. Selected bond lengths and angles are listed in Table 2.

Both compounds show an analogous structure, crystallizing in the triclinic space group $P\bar{1}$. The Mn^{II} ions are bridged by two $\mu_{1,3}$-carboxylate ligands in a *syn–anti* mode, with a Mn···Mn distance of ~ 4.72 Å. The hexacoordination of each manganese ion is completed by two phen ligands, leading to a distorted octahedral environment around Mn^{II} ions, with Mn–O distances much shorter than Mn–N distances (av. 2.136 and 2.266 Å for compound **1** and 2.140 and 2.259 Å for compound **2**, respectively). All distances agree with those reported for analogous compounds.[8–10]

Compound **1** shows π-stacking between phen ligands of neighbouring molecules, leading to chains (Fig. 3). These chains are interconnected through ClO_4^- anions and CH_3CN molecules *via* hydrogen bonds, generating a 3D system. Although compound

Table 2 Selected bond lengths (Å) and angles (°) with standard deviations in parentheses for compounds **1** and **2**

1·6CH$_3$CN		**2**·2CH$_3$CH$_2$OH	
Mn(1)···Mn(1a)	4.726(5)	Mn(1)···Mn(1b)	4.712(2)
Mn(1)–N(1)	2.2420(16)	Mn(1)–N(4)	2.2473(14)
Mn(1)–N(12)	2.2898(16)	Mn(1)–N(3)	2.2822(14)
Mn(1)–N(15)	2.2734(15)	Mn(1)–N(1)	2.2527(14)
Mn(1)–N(26)	2.2602(16)	Mn(1)–N(2)	2.2527(15)
Mn(1)–O(31a)	2.1381(13)	Mn(1)–O(2b)	2.1441(12)
Mn(1)–O(29)	2.1342(12)	Mn(1)–O(1)	2.1364(12)
O(31a)–Mn(1)–N(15)	167.64(5)	O(2b)–Mn(1)–N(1)	168.38(5)
O(29)–Mn(1)–N(12)	162.23(6)	O(1)–Mn(1)–N(3)	163.59(5)
N(1)–Mn(1)–N(26)	163.09(6)	N(4)–Mn(1)–N(2)	168.99(6)

Symmetry codes: (a) $-x, -y+1, -z+1$, (b) $-x+1, -y+1, -z+2$.

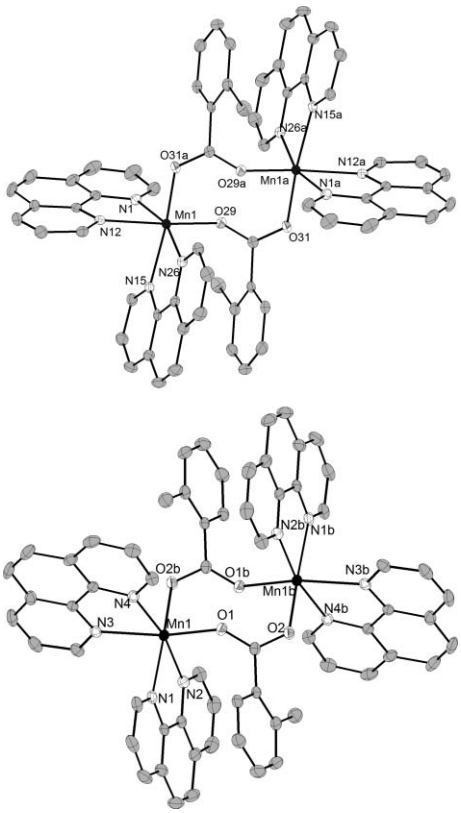

Fig. 2 Crystal structures of the cationic complexes of compounds **1** (top) and **2** (bottom), showing the atom labelling scheme and ellipsoids at 50% probability. Hydrogen atoms are omitted for clarity. Symmetry codes: (a) $-x, -y+1, -z+1$, (b) $-x+1, -y+1, -z+2$.

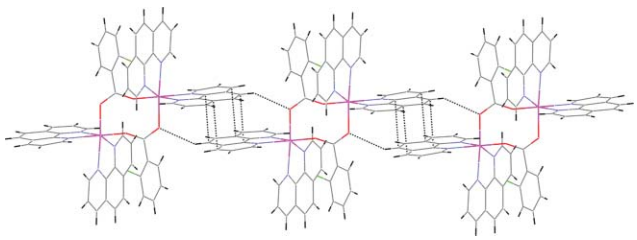

Fig. 3 π-stacking between phen ligands of dinuclear units of compound **1** generating chains.

2 displays structural parameters very similar to compound **1**, the interactions between molecules are different. Compound **2** also shows π-stacking between phen ligands of neighbouring complexes to generate chains, but these interactions are offset in this case (Fig. S1, ESI†). Moreover, there are C–H···π interactions between phen ligands of neighbouring molecules, leading to chains in another direction. The presence of ClO_4^- anions (with two disordered oxygen atoms) and CH_3CH_2OH molecules form the 3D system.

[{Mn(phen)$_2$}$_2$(μ-3-ClC$_6$H$_4$COO)$_2$](ClO$_4$)$_2$ (3), [{Mn(phen)$_2$}$_2$(μ-3-CH$_3$C$_6$H$_4$COO)$_2$](ClO$_4$)$_2$ (4), [{Mn(phen)$_2$}$_2$(μ-4-ClC$_6$H$_4$COO)$_2$](ClO$_4$)$_2$ (5) and [{Mn(phen)$_2$}$_2$(μ-4-CH$_3$C$_6$H$_4$COO)$_2$](ClO$_4$)$_2$ (6). The cationic complexes of **3** and **4** are shown in Fig. 4 and those of **5** and **6** in Fig. 5. Selected bond lengths and angles are given in Table 3 (compounds **3** and **4**) and Table 4 (compounds **5** and **6**). Compounds **3** and **4** crystallize in the

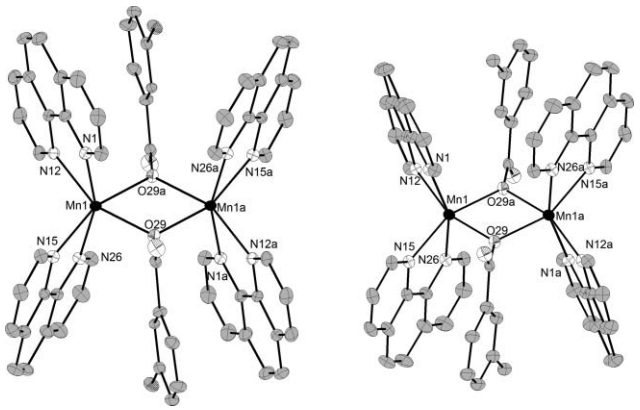

Fig. 4 Crystal structures of the cationic complexes of compounds **3** (left) and **4** (right), showing the atom labelling scheme and ellipsoids at 50% probability. Hydrogen atoms are omitted for clarity. Symmetry codes: (a) 1–*x*, –*y*,1–*z*.

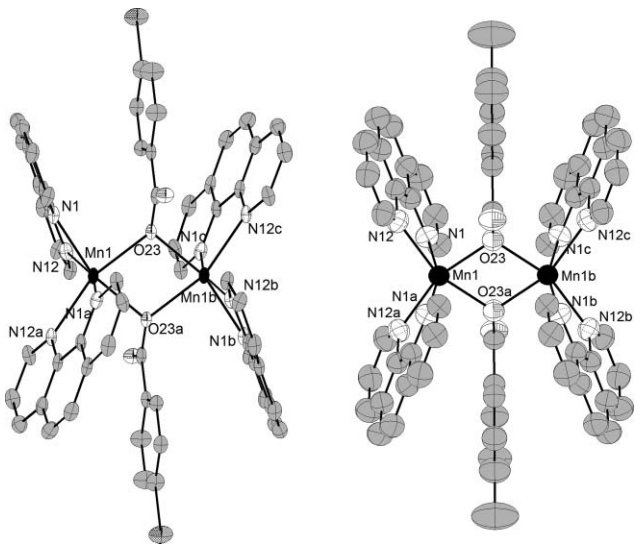

Fig. 5 Crystal structures of the cationic complexes of compounds **5** (left) and **6** (right), showing the atom labelling scheme and ellipsoids at 50% probability. Hydrogen atoms are omitted for clarity. Symmetry codes: (a) –*x*, *y*, –*z*, (b) –*x*,1–*y*, –*z*, (c) *x*,1–*y*, *z*.

triclinic space group $P\bar{1}$ while compounds **5** and **6** crystallize in the monoclinic space group *C*2/*m*. All compounds show an analogous structure. Each Mn^{II} ion coordinates two phen and two carboxylate ligands, which bridge both Mn^{II} ions in a very uncommon coordination mode: the $\mu_{1,1}$. The Mn···Mn distance is ~ 3.45 Å, much shorter than those for compounds **1** and **2** (~ 4.72 Å), in agreement with the different bridging mode. As has been said, the carboxylate ligands act as monatomic bridges, with $Mn–O_{bridge}$ distances of ~ 2.19 Å, slightly larger than those for compounds **1** and **2** (~ 2.14 Å). The Mn_2O_2 core is a planar rhombus, with $Mn–O_b–Mn$ angles of ~ 105° for compounds **3** and **4** and slightly smaller for compounds **5** and **6** (~ 103°). The torsion angles between the phenyl rings and the carboxylate groups are very small (even 0° for compounds **5** and **6**), meaning that the benzoate rings are perpendicular to the Mn_2O_2 plane.

Compound **3** displays disorder in the 3-chlorobenzoate rings, with occupancies of 0.5205 (A atoms) and 0.4795 (B atoms). The

Table 3 Selected bond lengths (Å) and angles (°) with standard deviations in parentheses for compounds **3** and **4**

	3	**4**
Mn(1)···Mn(1a)	3.469(1)	3.454(2)
Mn(1)–N(1)	2.2563(11)	2.256(2)
Mn(1)–N(12)	2.2596(11)	2.263(2)
Mn(1)–N(15)	2.2412(11)	2.244(2)
Mn(1)–N(26)	2.2655(11)	2.266(2)
Mn(1)–O(29)	2.1667(9)	2.2010(16)
Mn(1)–O(29a)	2.2065(10)	2.1637(16)
O(29)–Mn(1)–N(12)	160.75(4)	160.26(7)
O(29a)–Mn(1)–N(15)	157.56(4)	157.63(7)
N(1)–Mn(1)–N(26)	159.90(4)	159.44(7)
O(29)–Mn(1)–O(29a)	75.03(4)	75.37(7)
Mn(1)–O(29)–Mn(1a)	104.97(4)	104.63(7)

Symmetry codes: (a) 1–*x*, –*y*,1–*z*.

Table 4 Selected bond lengths (Å) and angles (°) with standard deviations in parentheses for compounds **5** and **6**

	5	**6**
Mn(1)···Mn(1b)	3.415(2)	3.460(1)
Mn(1)–O(23)	2.189(4)	2.1991(16)
Mn(1)–N(1)	2.262(5)	2.280(2)
Mn(1)–N(12)	2.237(6)	2.267(2)
N(12)–Mn(1)–O(23a)	161.68(15)	160.44(8)
N(1)–Mn(1)–N(1a)	161.55(21)	160.72(11)
O(23)–Mn(1)–O(23a)	77.46(0)	76.24(10)
Mn(1)–O(23)–Mn(1b)	102.54(1)	103.76(10)

Symmetry codes: (a) –*x*, *y*, –*z*, (b) –*x*,1–*y*, –*z*.

dinuclear units interact by π-stacking between phen ligands and phenyl rings of neighbouring molecules and C–H···π interactions leading to layers (Fig. 6), which are interconnected *via* ClO_4^- anions generating the 3D system. Compound **4** displays 50% disorder in the 3-methylbenzoate rings. This is not a thermal disorder but structural, as both possibilities can not coexist due to steric hindrance. This compound also shows π-stacking between phen ligands of neighbouring dinuclear units, generating chains. The presence of ClO_4^- anions lead to the 3D system *via* hydrogen bonds (Fig. S2, ESI†). Compound **5** displays disorder in the ClO_4^- anions. The dinuclear complexes form chains through C–H···Cl interactions of 4-chlorobenzoate ligands of neighbouring molecules (Fig. 7a). These chains are interconnected *via* π-stacking between phen ligands of neighbouring chains (Fig. 7b). The 3D system is obtained by C–H···O interactions (Fig. 7c) and interactions between the dinuclear units and the ClO_4^- anions. Compound **6** also displays disorder in the ClO_4^- anions, but just in the oxygen atoms. The dinuclear complexes can form chains in all three directions through hydrogen bonds between phen ligands and perchlorate anions, leading to a 3D system (Fig. S3, ESI†).

The $\mu_{1,1}$-bridging mode is found in several trinuclear Mn^{II} complexes with a $[Mn_3(RCOO)_6]$ core.[19] However in that case, there is usually at least a weak interaction between the non-coordinated oxygen atom and the terminal Mn^{II} ions as they do not complete their hexacoordination. A study made by Lippard considered the distance between the non-coordinated or dangling oxygen and the Mn^{II} ions as a distinctive parameter of the monodentate bridging.[21] This distance is ~ 3.84 Å for compounds **3** and **4** and ~ 3.77 Å for compounds **5** and **6**, too large for an interaction,

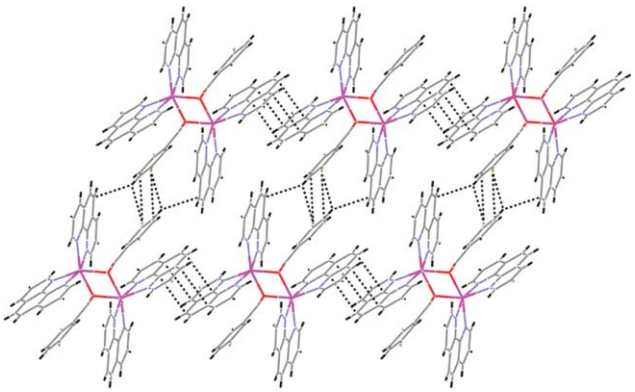

Fig. 6 π-stacking and C–H···π interactions between dinuclear units of compound **3**.

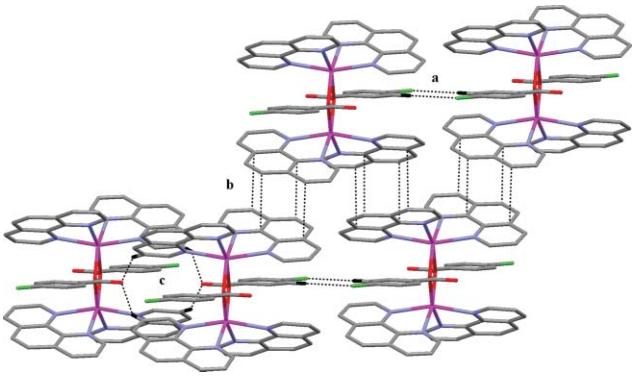

Fig. 7 C–H···Cl interactions (**a**), π-stacking (**b**) and C–H···O interactions (**c**) between dinuclear units of compound **5**. Only hydrogen atoms involved in contacts are not omitted.

which indicate that these four compounds reported here represent dinuclear Mn^{II} complexes containing pure monodentate bridging carboxylates. Moreover, in these compounds, the Mn^{II} ions are already hexacoordinated.

As has been indicated, dinuclear Mn^{II} compounds displaying this type of bridging mode are found in very few cases, the carboxylate group usually forming part of polydentate ligands, which are not comparable because they may possibly adopt this coordination mode due to steric hindrance or preferences for other coordinating atoms. There are just three dinuclear compounds reported in the literature similar enough to compare the structural parameters.[13] The compounds reported here (**3–6**) show the shortest Mn···Mn distance, with a value of ~ 3.45 Å, which is outside the range 3.525–3.589 Å. They also display a large C–O_b distance, ~ 1.31 Å compared to the range 1.165–1.281 Å, and a very large Mn–O_d distance, ~ 3.80 Å in comparison with the range 3.405–3.538 Å. All the other distances and angles agree with those reported in the literature.

Magnetic properties

Magnetic susceptibility data were recorded for all compounds (**1–6**) from room temperature to 2 K. $\chi_M T$ *vs.* T and χ_M *vs.* T plots of compounds **1** and **2** are displayed in Fig. 8. Both compounds show analogous magnetic behavior. At 300 K, the $\chi_M T$ values are 9.21 and 8.59 $cm^3\ mol^{-1}\ K$ for compounds **1** and **2** respectively, close to the typical value for two uncoupled Mn^{II} ions ($S = 5/2$, 8.75 $cm^3 mol^{-1} K$ assuming $g = 2$). As the temperature decreases, the $\chi_M T$ values fall until reaching 0.92 (**1**) and 1.05 $cm^3\ mol^{-1}\ K$ (**2**) at 2 K, indicative of an antiferromagnetic coupling. This behavior is also observed in χ_M *vs.* T plots (inset Fig. 8). At 300 K, χ_M values are 0.03 $cm^3\ mol^{-1}$ for both compounds, increasing with temperature until reaching a maximum of 0.50 $cm^3\ mol^{-1}$ at ~ 5.5 K for compound **1** and 0.37 $cm^3 mol^{-1}$ at ~ 6.0 K for compound **2**. The experimental data were fitted by using the spin Hamiltonian $H = -JS_1 \cdot S_2$ and the corresponding susceptibility expression for two high spin Mn^{II} ions.[22] For compound **1**, the best fit for $\chi_M T$ (and χ_M) data was obtained with $J = -1.41$ (-1.30) cm^{-1}, $g = 2.05$ (2.01) and $R = 1.07 \times 10^{-4}$ (1.41×10^{-4}). For compound **2**, the best fit for $\chi_M T$ (and χ_M) data was obtained with $J = -1.66$ (-1.71) cm^{-1}, $g = 2.00$ (1.98) and $R = 6.47 \times 10^{-4}$ (9.25×10^{-4}). These J values agree with the range ~ 0 to -1.94 cm^{-1} found in the literature for other Mn^{II} compounds with two *syn–anti* carboxylate bridges.[9j,10b–e]

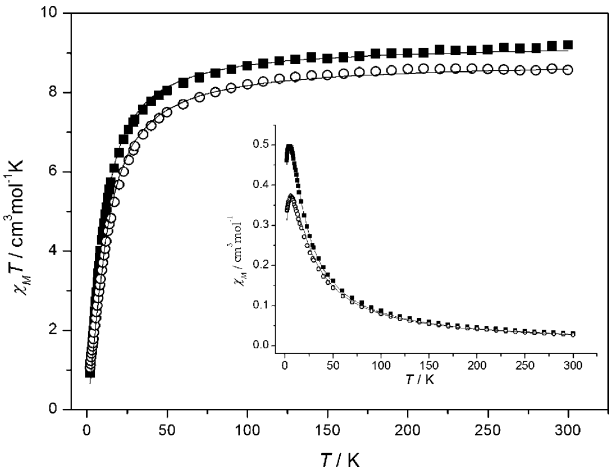

Fig. 8 $\chi_M T$ *vs.* T and χ_M *vs.* T (inset) plots for compounds **1** (■) and **2** (○). The solid line is the best fit to the experimental data.

There are two kinds of compounds reported in the literature where the Mn^{II} ions are bridged only through two carboxylate ligands coordinated in a *syn–anti* mode: dinuclear complexes and one-dimensional systems. Table 5 summarize the most important structural data for these compounds and their magnetic coupling constants.

All compounds show a weak (or negligible) antiferromagnetic coupling, with J values between 0 and -2 cm^{-1}. The difference between these compounds is in the RCOO bridge and/or the capping ligand (phen, bpy or tpa). Therefore, there are two factors that could affect the magnetic properties: the electronic effects due to the different carboxylate bridge and the structural parameters. It is interesting to note that compounds **1** and **D**, with the same 2-ClC_6H_4COO bridging ligand, show different degrees of magnetic coupling, the compound with bpy being a little more antiferromagnetic. These compounds show appreciable differences in their structural parameters. On the other hand, the one-dimensional systems **G** and **H**, with the same 3-ClC_6H_4COO bridging ligand, show similar J values, in agreement with the similarity of their structural parameters. The difference between the one-dimensional systems and the dinuclear complexes is the presence of one (in 1D systems) or two (in the dinuclear complexes) bidentate capping ligands coordinated to the Mn^{II} ions. The coordination of two phen ligands, more rigid than bpy ligands,

Table 5 Selected structural and magnetic data for Mn^{II} systems with a $[Mn_2(\mu\text{-}RCOO)_2]^{2+}$ core

Compound[a]		d_{anti}[b]	d_{syn}[c]	α[d]	β[e]	J[f]/cm^{-1}	Ref
Dinuclear complexes							
$[Mn_2(ClCH_2COO)_2(phen)_4](ClO_4)_2$	**A**	2.129	2.150	99.9	138.2	0	10d
$[Mn_2(Hphth)_2(phen)_4](Hphth)_2$	**B**	2.134	2.118	94.7	128.3	–0.34	10c
$[Mn_2(2\text{-}ClC_6H_4COO)_2(phen)_4](ClO_4)_2$	**1**	2.134	2.138	94.26	123.89	–1.41	this work
$[Mn_2(2\text{-}CH_3C_6H_4COO)_2(phen)_4](ClO_4)_2$	**2**	2.137	2.144	95.8	127.4	–1.66	this work
$[Mn_2(\mu\text{-}C_6H_4COO)_2(bpy)_4](ClO_4)_2$	**C**	2.139	2.118	103.6	151.9	–1.76	10e
$[Mn_2(\mu\text{-}2\text{-}ClC_6H_4COO)_2(bpy)_4](ClO_4)_2$	**D**	2.199	2.117	96.4	130.9	–1.79	9j,10e
$[Mn_2(CH_3COO)(tpa)](TCNQ)_2$	**E**	2.160	2.060	107.6	133.5	–1.94	10b
1D systems							
$[Mn(ClCH_2COO)_2(phen)]_n$	**F**	2.183	2.134	97.9	123.9	–0.89	10d
$[Mn(bpy)(3\text{-}ClC_6H_4COO)_2]_n$	**G**	2.196	2.104	100.5	134.4	–1.72	10e
$[Mn(3\text{-}ClC_6H_4COO)_2(phen)]_n$	**H**	2.200	2.091	100.4	136.1	–1.80	19

[a] Compounds: Hphth = monodeprotonated phthalate; tpa = tris(2-pyridylmethyl)-amine; TCNQ = tetracyanoquinodimethane. [b] Mn–O_{anti} distance. [c] Mn–O_{syn} distance. [d] O_{anti}–Mn–O_{syn} angle. [e] Mn–O_{syn}–C angle. [f] Magnetic exchange coupling parameter based on the Hamiltonian $H = -JS_1 \cdot S_2$.

could explain the greater distortion of the octahedral coordination and, consequently, more differences in the structural parameters of the carboxylate bridges.

$\chi_M T$ *vs.* T plots of the remaining dinuclear Mn^{II} compounds are depicted in Fig. 9 (compounds **3** and **4**) and Fig. 10 (compounds **5** and **6**). All compounds show analogous magnetic behavior. At 300 K, the $\chi_M T$ values are 9.41, 9.55, 8.89 and 9.28 cm^3 mol^{-1} K for compounds **3–6** respectively, close to the expected value for two uncoupled high spin Mn^{II} ions ($S = 5/2$, 8.75 cm^{3}mol^{-1}K assuming $g = 2$).

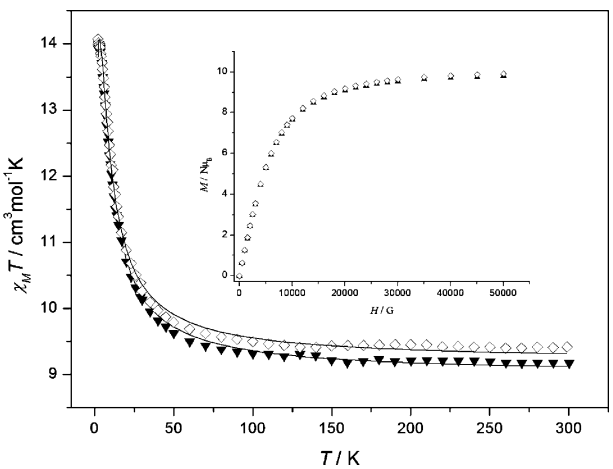

Fig. 9 $\chi_M T$ *vs.* T and M *vs.* H (inset) plots for compounds **3** (▲) and **4** (◇). The solid line is the best fit to the experimental data.

As the temperature decreases, the $\chi_M T$ values increase until reaching a maximum value of 14.00 cm^3 mol^{-1} K at 2.5 K (**3**), 14.01 cm^3 mol^{-1} K at 2.5 K (**4**), 13.00 cm^3 mol^{-1} K at 3.0 K (**5**) and 13.75 cm^3 mol^{-1} K at 2.7 K (**6**). Below this temperature, $\chi_M T$ values fall slightly. This behavior is characteristic of ferromagnetic coupling, which is confirmed by the field dependence of the magnetization at 2 K, showing $M/N\mu_B$ values indicative of ten unpaired electrons (insets Fig. 9 and Fig. 10). The $\chi_M T$ expected value for a system with a ground state $S = 5$ is 15 cm^3 mol^{-1} K; the lower values found at ~ 2.5 K and the decreasing of $\chi_M T$ below this temperature could be explained by the existence of intermolecular antiferromagnetic interactions or the zero-field splitting (ZFS) of the ground state. In

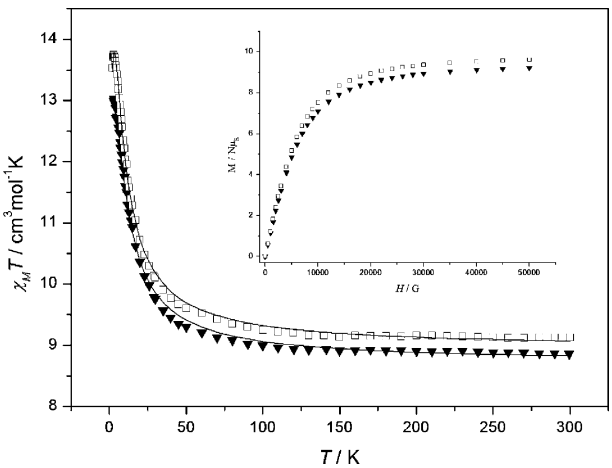

Fig. 10 $\chi_M T$ *vs.* T and M *vs.* H (inset) plots for compounds **5** (▼) and **6** (□). The solid line is the best fit to the experimental data.

Table 6 Parameters obtained from the fit of $\chi_M T$ data of compounds **3–6**

Compound	J/cm^{-1}	zJ'/cm^{-1}	g	R
3	1.01	–0.015	2.03	1.93×10^{-5}
4	0.98	–0.019	2.05	5.01×10^{-5}
5	1.04	–0.026	1.99	4.65×10^{-5}
6	1.06	–0.018	2.02	3.12×10^{-5}

this case, the experimental data were fitted by using the spin Hamiltonian $H = -JS_1 \cdot S_2$ and taking into account intermolecular interactions (zJ');[23] the best fit parameters obtained are listed in Table 6.

As has been indicated, there are very few dinuclear compounds with Mn^{II} ions bridged through two $\mu_{1,1}$-carboxylate ligands analogous to those reported here, just three, and none of them is magnetically characterized. Regarding other dinuclear complexes with the same core but where the carboxylate bridges belong to polydentate ligands, only three of them show hexacoordinated Mn^{II} ions, these compounds displaying weak antiferromagnetic coupling.[12a–c] However, as is shown in Table 7, there are four 1D systems which consist of dinuclear entities with the $[Mn_2(\mu_{1,1}\text{-}RCOO)_2]^{2+}$ core interconnected by long ligands. These compounds show ferromagnetic coupling, with J values in the range 0.92–1.80 cm^{-1}.[14c–e]

Table 7 Selected structural and magnetic data for Mn^{II} compounds with a $[Mn_2(\mu\text{-}O)_2]$ core

	Compound[a]	Mn–O_b–Mn/°	Mn···Mn/Å	Mn–O_b[b]/Å	τ[c]/°	J[d]/cm^{-1}	Ref
	3	104.97	3.469	2.187	0	1.01	this work
	4	104.63	3.454	2.182	0	0.98	this work
	5	102.54	3.415	2.189	0	1.04	this work
	6	103.76	3.460	2.199	0	1.06	this work
	Carboxylate in polydentate ligand						
A	$[Mn_2(Hbida)_2(H_2O)_2]$	104.92	3.446	2.173	0	–0.94	12a
B	$[Mn_2(H_2O)_4L_2]$	108.38	3.672	2.281	0.07	–0.96	12b
C	$[Mn_2(H_2O)_6(HL)_2]$	105.99	3.472	2.174	0	–2.60	12c
	1D systems						
D	$[Mn(oba)(phen)(H_2O)]_n$	101.81	3.387	2.182	0	0.92	14c
E	$[Mn(HBTC)(H_2O)L]_n$	104.23	3.489	2.211	0	1.44	14d
F	$[Mn(HBTC)(H_2O)L]_n$	104.39	3.482	2.204	0	1.46	14d
G	$[Mn(HBTC)(bpy)(H_2O)]_n$	105.10	3.507	2.209	0	1.80	14e
	Alkoxo/phenoxo						
H	$[Mn_2(H_2L1)(CH_3COO)_2]$	103.66	3.346	2.128	0	> 0[e]	25a
I	$[Mn_2(H_2L)_2Cl_2]$	105.37	3.443	2.165	0	0.62	25b
J	$[Mn_2(CH_3COO)_2L]$	102.96	3.367	2.152	0	0.80	25c
K	$[Mn(ema)_2(H_2O)]_2$	102.67	3.394	2.173	0	1.00	25d
L	$(TMA)_2[Mn_2L_2]$	101.48	3.332	2.152	0.34	1.04	25e
M	$[Mn_2(py2ald)_2](ClO_4)_2$	104.89	3.401	2.145	16.38	1.14	25f
N	$[Mn(bpeap)(THF)]_2(ClO_4)_2$	99.90	3.256	2.126	0	<–0.18[f]	25g
O	$[Mn_2L1L2](BPh_4)_2$	100.27	3.280	2.137	11.77	–1.50	25h
P	$[Mn(SALPS)]_2$	101.28	3.299	2.134	8.13	–1.88	25i
Q	$[Mn_2L_2](ClO_4)_2$	103.68	3.383	2.152	17.9	–3.20	25j
R	$[Mn_2L](ClO_4)_2$	102.57	3.518	2.255	25.48	–4.52	25k
	***N*-oxide**						
S	$[Mn(hfac)_2(4\text{-}cpyNO)]_2$	107.01	3.567	2.218	0	0.23	26a
T	$[Mn_2(dmpo)_4(SCN)_4(H_2O)_2]$	109.00	3.599	2.211	0	–1.09	26b
U	$[Mn(hfac)_2(IMHF)]_2$	105.88	3.476	2.178	0	–1.72	26c
V	$[Mn(hfac)_2AmPh]_2$	105.76	3.465	2.174	0	–1.99	26d
W	$[Mn(hfac)_2(IMHBithph)]_2$	107.03	3.510	2.183	0.47	–3.10	26e
	Phosphonate						
X	$[Mn_2(bbimp)_2(H_2O)_2]$	102.80	3.358	2.149	0	1.44	27

[a] **A**, H_3bida = N-(benzimidazol-2-ylmethyl)iminodiacetic acid; **B**, L = N,N-bis[(1-methylimidazol-2-yl)-methyl]glycinate; **C**, H_3L = 2,6-dioxo-l,2,3,6-tetrahydropyrimidine-4-carboxylic acid; **D**, Hoba = 4,4′-oxybis(benzoic) acid; **E**, H_3BTC = benzene-1,3,5-tricarboxylic acid and L = pyridine-2-(1-methyl-1*H*-pyrazol-3-yl); **F**, L = pyridine-2-(1-methyl-4-bromo-1*H*-pyrazol-3-yl); **H**, H_2L1 = bis(2,6-bis((2-hydroxypropyl-1,3-di-imino)methyl)-4-methylphenolate); **I**, H_3L = N-(2-hydroxy-5-nitrobenzyl-iminodiethanol); **J**, L = 11,23-dimetyl-25,26-dioxo-3,7,15,19-tetra-azatricyclo-hexacosa-1,2,7,9,11,13,14,19,21-decane; **K**, Hema = 2-ethyl-3-hydroxy-4-pyrone; **L**, L = 1,3-bis(5-nitrosalicylideneimino)-2-propanolate; **M**, py2ald = 6-(bis(pyrid-2-ylmethyl)aminomethyl)-2-formyl-4-methylphenolato; **N**, bpeap = bis(o-(bis(2-(1-pyrazolyl)ethyl)amino)phenolate); **O**, L1 = 1-(2-Pyridylmethylamino)-2-((2-oxybenzyl)(2-pyridylmethyl)amino)ethane), L2 = (1-(2-pyridylmethyleneamino)-2-((2-oxybenzyl)(2-pyridylmethyl)amino)ethane); **P**, SALPS = N,N′-[1,l′-dithiobis(phenylene)]bis(salicylideneaminate); **Q**, L = N,N′-ethylene-*N*-(bis(2-pyridylmethyl)amino)-*N*′-(eliminatedeneiminate); **R**, L = bis((2,6-diformyl-4-chlorophenolate)-*N*,*N*′-(3-((2-pyridylmethyl)aminoethyl)-1,5-diamino3-azapentane))); **S**, hfac = hexafluoroacetylacetonate and 4-cpyNO = 4-cyanopyridine-*N*-oxide; **T**, dmpo = 3,5-dimethylpyridine-*N*-oxide; **U**, IMHF = 1-hydroxo-2-furfural-4,4,5,5-tetramethyl-4.5-dihydro-1*H*-imidazole; **V**, AmPh = 2-phenyl-4,4,5,5-tetramethylimidazoline-3-oxide; **W**, IMHBithph = 1-hydroxy-2-bithiophenal-4,4,5,5-tetramethyl-4,5-dihydro-1*H*-imidazole and NIT2-bithph = 4,4,5,5-tetramethyl-2-(bithiophenal-2-yl)imidazoline-1-oxyl-3-oxide; **X**, bbimp = bis(benzimidazol-2-ylmethyl)imino(methylenphosphonate). [b] Average values. [c] Mn–O–Mn–O angle. [d] Magnetic exchange coupling parameter based on the Hamiltonian $H = -JS_1 \cdot S_2$. [e] Ferromagnetic behavior observed but not fitted. [f] The authors give this J value based on T_{max} is less than 1.5 K.

The analysis of the ferromagnetic chain $[Mn^{II}(oba)(phen)(H_2O)]_n$,[14c] which shows two monatomic bridges between Mn^{II} ions, reported by Wang *et al.*[24] concluded that angles ~ 103° could favour the ferromagnetic coupling for this kind of compound. This agrees with experimental observations, where analogous compounds with angles ~ 104° show ferromagnetic coupling (Table 7).

Taking into consideration the $\mu_{1,1}$-coordination mode of the carboxylate, the magnetic interaction in these compounds is due to the $[Mn_2(\mu\text{-}O)_2]^{2+}$ core. Thus, with the aim of finding magneto-structural correlations, dinuclear complexes with other monatomic oxo ligands, such as alkoxo/phenoxo,[25] *N*-oxide[26] and phosphonate,[27] are also included in Table 7. Compounds with alkoxo/phenoxo bridges show ferro- or antiferromagnetic behavior, with J values between +1.2 cm^{-1} and –4.5 cm^{-1}. Nevertheless, most of these compounds show a non-planar core, in contrast to compounds with $\mu_{1,1}$-RCOO bridges reported here. Compounds with *N*-oxide as a bridging ligand also display ferro- or antiferromagnetic interactions (J values between +0.23 and –3.1 cm^{-1}) and only one them shows a non-planar $[Mn_2O_2]$ core. There is also one compound reported in the literature with two phosphonate bridges, which displays ferromagnetic coupling between the Mn^{II} ions in the planar core.

A linear relationship between the structural parameters of compounds reported in Table 7 can be observed: the Mn···Mn distance increases with the Mn–O_b–Mn angle, as well as with the Mn–O_b distance (Fig. S4–S5, ESI†). A best correlation is found when only systems with planar core are considered. Nevertheless, no clear magneto-structural correlation could be established for these compounds. Complexes with two $\mu_{1,1}$-carboxylate bridges, like **3–6**, as well as other compounds with a $[Mn_2(\mu\text{-}O)_2]^{2+}$ core, show similar structural parameters and small J values in all cases, the magnetic behavior being ferro- or antiferromagnetic.

The $[Mn_2(\mu\text{-}O)_2]^{n+}$ core is also found in Mn_2^{IV} and $Mn^{III}Mn^{IV}$ compounds, but they show a strong antiferromagnetic behavior. The dramatic change in their magnetic behavior, compared to the Mn_2^{II} systems could be due to structural differences. In these systems, the Mn–O_b and the Mn···Mn distances (~ 1.8 and ~ 2.8 Å, respectively) are around 10–20% shorter than those found for Mn^{II} compounds (~2.2 and ~ 3.4 Å, respectively). Moreover, the Mn–O_b–Mn angle is also smaller (~ 96° in contrast with ~ 104° for Mn^{II} complexes). DFT studies of high-valence $[Mn_2(\mu\text{-}O)_2]^{n+}$ systems, reported by Ruiz–Garcia *et al.*,[28] reveal that in these compounds the magnetic coupling is dominated by the in-plane $d_{x^2-y^2}$ type superexchange pathway *via* the oxo bridges with a small, but non negligible, contribution from direct $d_{x^2-y^2}$ type Mn···Mn σ-bond. For Mn^{II} complexes, with larger Mn···Mn distances, the degree of this overlap must be very small and the $d_{x^2-y^2}/d_{x^2-y^2}$ interaction would be only through the bridge, decreasing drastically the antiferromagnetic contribution. Moreover, the presence of two more electrons in each manganese ion provides additional pathways ($d_{xy}/d_{x^2-y^2}$ and d_{xy}/d_{xy}) which could be ferromagnetic or weak antiferromagnetic contributions depending on structural parameters.

EPR spectra

EPR spectra of compounds **1–6** were recorded on powdered samples at different temperatures. At room temperature all complexes show a broad band centered at $g \sim 2$ although at low temperatures the spectra of ferro- and antiferromagnetic compounds are considerably different. For ferromagnetic compounds (**3–6**), the shape of the spectra at room temperature is similar to those at 4 K, only the band width changes a little on cooling and small features appear at ~ 155 and ~ 250 G (Fig. 11). In contrast, for the antiferromagnetic compounds (**1** and **2**) the shape of the spectra is very sensitive to temperature, showing at 4 K two more bands at both sides of g ~2 and other features at lower fields (Fig. 12).

Compounds with ferromagnetic coupling show a spin ground state $S = 5$, while for compounds displaying antiferromagnetic coupling the spin ground state is $S = 0$. Although at 4 K the latter compounds should be EPR silent, the small J values allow the lowest excited states $S = 1$ and $S = 2$ to be populated.

The spectra at 4 K of all compounds were simulated with the easyspin software[15] by considering a dinuclear system of two $S = 5/2$ ions with the magnetic exchange interaction (J) obtained from the magnetic data and including the ZFS parameters of the single ion (D_{Mn} and E_{Mn}). All simulations were performed with $g = 2.0$. Fairly good simulations were achieved with D and E values of 0.090 and 0.030 cm^{-1} (**1**), 0.100 and 0.020 cm^{-1} (**2**), 0.060 and 0.005 cm^{-1} (**3**), 0.070 and 0.005 cm^{-1} (**4**), 0.045 and 0.002 cm^{-1} (**5**) and 0.065 and 0.002 cm^{-1} (**6**). These values agree with the small distortions characteristic of Mn^{II} ions.

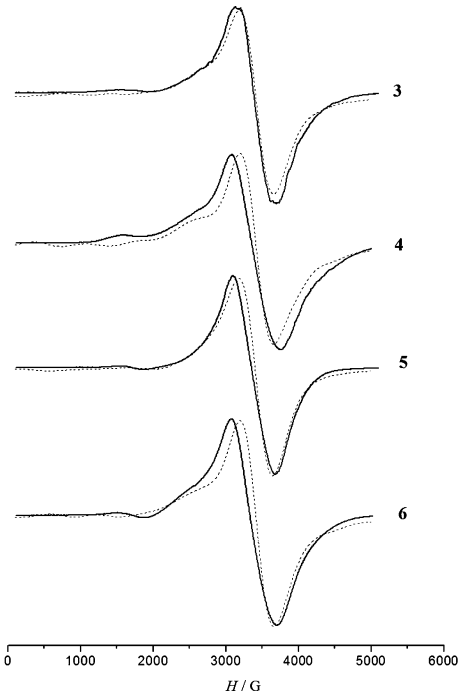

Fig. 11 X-band EPR spectra of powdered samples of the ferromagnetic dinuclear compounds **3–6** at 4 K. The dashed line is the best simulation achieved.

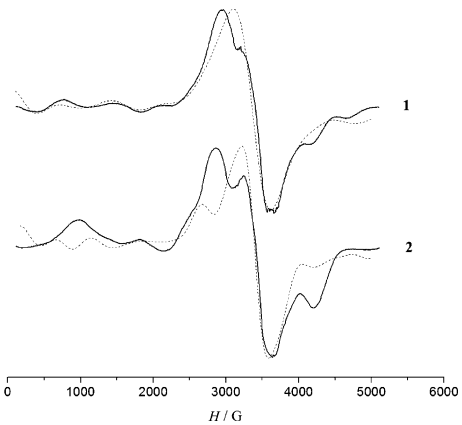

Fig. 12 X-band EPR spectra of powdered samples of the antiferromagnetic dinuclear compounds **1** and **2** at 4 K. The dashed line is the best simulation achieved.

As can be observed, compounds **1** and **2**, with a ground state of $S = 0$, show appreciably larger D and E values than compounds **3–6**, with a ground state of $S = 5$, despite displaying quite similar structural parameters. It is well known that the ZFS has two contributions: dipolar and anisotropic interactions. For dinuclear Mn^{II} compounds the cofficient for these contributions to the D_S value is very different for $S = 5$ and $S = 1$: $D_5 = (4/9)D_{Mn} + (5/18)D_{dip}$ while $D_1 = (-32/5)D_{Mn} + (37/10)D_{dip}$.[23] Therefore, the $S = 1$ state is more sensitive to both contributions than the $S = 5$, and consequently more complex spectra should be obtained for the antiferromagnetic systems than for the ferromagnetic ones, as is observed experimentally.

In the simulation of the spectra, a phenomenological D value has been considered, which does not include the dipole–dipole interactions. However, it is possible that this contribution is non-negligible.[29] The dipolar interaction is proportional to r^{-3}, r being the distance between the paramagnetic centers. The Mn···Mn distance in the ferromagnetic compounds is appreciably shorter than in the antiferromagnetic ones, so the dipolar contribution should be more important for complexes **3–6** than for complexes **1** and **2**.

Summarizing, the EPR spectra for this kind of dinuclear complex is a tool for differentiating between ferro- and antiferromagnetic compounds. For the antiferromagnetic complexes, with large Mn···Mn distances, the dipolar contribution to the ZFS should be small, and the D and E values proposed from the simulation can well describe the system. However, for the ferromagnetic compounds, the situation is more complex due to the small contributions of the dipolar and anisotropic interactions. Moreover, due to the short Mn···Mn distance, the dipolar contribution is not negligible. Therefore, D and E values for the ferromagnetic compounds must be taken into consideration with caution.

Conclusions

Six new dinuclear Mn^{II} compounds have been synthesized and structurally and magnetically characterized. Compounds **1** and **2** show two $\mu_{1,3}$-carboxylate bridges in a *syn–anti* mode while compounds **3–6** present two $\mu_{1,1}$-carboxylate bridges. This difference in the coordination mode of the carboxylate ligands affects the magnetic behavior in such a way that compounds **1** and **2** display antiferromagnetic interactions and compounds **3–6** ferromagnetic interactions. This ferromagnetic behavior, compared to the antiferromagnetic interaction found for Mn^{IV} compounds with the same core, is due to the large Mn···Mn distance and the Mn–O_b–Mn angle, which make the J_{AF} interactions diminish. Moreover, the different magnetic behavior is also reflected in the EPR spectra, where antiferromagnetic compounds (**1** and **2**) show much more complicated EPR spectra at 4 K than ferromagnetic compounds (**3–6**).

Acknowledgements

This work was supported by the Ministerio de Ciencia e Innovación of Spain through the project CTQ2009-07264/BQU, the Comissió Interdepartamental de Recerca i Innovació Tecnològica of la Generalitat de Catalunya (CIRIT) (2009-SGR1454). V.G. thanks the Ministerio de Ciencia e Innovación for the PhD grant BES-2007-15668.

Notes and references

1 M. Murrie and D. J. Price, *Annu. Rep. Prog. Chem., Sect. A*, 2007, **103**, 20 and references cited therein.
2 A. J. Wu, J. E. Penner-Hahn and V. L. Pecoraro, *Chem. Rev.*, 2004, **104**, 903.
3 C. S. Mullins and V. L. Pecoraro, *Coord. Chem. Rev.*, 2008, **252**, 416.
4 See for examples: J. Vicario, R. Eelkema, W. R. Browne, A. Meetsema, R. M. La Crois and B. L. Feringa, *Chem. Commun.*, 2005, 3936; N. Nakasuka, S. Azuma, C. Katayama, M. Honda, J. Tanaka and M. Tanaka, *Acta Crystallogr., Sect. C: Cryst. Struct. Commun.*, 1985, **41**, 1176; Y. Journaux, T. Glaser, G. Steinfeld, V. Lozan and B. Kersting, *Dalton Trans.*, 2006, 1738; S. Sain, T. K. Maji, G. Mostafa, T.-H. Lu and N. R. Chaudhuri, *Inorg. Chim. Acta*, 2003, **351**, 12; T. M. Becker, J. J. Alexander, J. A. Krause Bauer, J. L. Nauss and F. C. Wireko, *Organometallics*, 1999, **18**, 5594.
5 See for examples: S. Blanchard, G. Blondin, E. Riviere, M. Nierlich and J.-J. Girerd, *Inorg. Chem.*, 2003, **42**, 4568; S.-B. Yu, S. J. Lippard, I. Shweky and A. Bino, *Inorg. Chem.*, 1992, **31**, 3502; U. P. Singh, P. Tyagi and S. Upreti, *Polyhedron*, 2007, **26**, 3625.
6 See for examples: I. Romero, L. Dubois, M.-N. Collomb, A. Deronzier, J.-M. Latour and J. Pecaut, *Inorg. Chem.*, 2002, **41**, 1795; Z. Chen, Y. Ma, F. Liang and Z. Zhou, *J. Organomet. Chem.*, 2008, **693**, 646; U. P. Singh, R. Singh, S. Hikichi, M. Akita and Y. Moro-oka, *Inorg. Chim. Acta*, 2000, **310**, 273.
7 See for examples: M. A. Kiskin, I. G. Fomina, G. G. Aleksandrov, A. A. Sidorov, V. M. Novotortsev, Y. V. Rakitin, Z. V. Dobrokhotova, V. N. Ikorsikii, Y. G. Shvedenkov, I. L. Eremenko and I. I. Moiseev, *Inorg. Chem. Commun.*, 2005, **8**, 89; M. Nakashima, H. Maruo, T. Hata and T. Tokii, *Chem. Lett.*, 2000, 1277.
8 (*a*) Q.-Z. Zhang and C.-Z. Lu, *Acta Crystallogr., Sect. C: Cryst. Struct. Commun.*, 2005, **61**, m78; (*b*) J. Chai, H. Zhu, H. W. Roesky, C. He, H.-G. Schmidt and M. Noltemeyer, *Organometallics*, 2004, **23**, 3284; (*c*) W.-H. Miao and L.-G. Zhu, *Acta Crystallogr., Sect. E: Struct. Rep. Online*, 2006, **62**, m1835; (*d*) J.-M. Yang, Z.-H. Zhou, H. Zhang, H.-J. Wan and S.-J. Lu, *Inorg. Chim. Acta*, 2005, **358**, 1841; (*e*) B. Moubaraki, K. S. Murray and E. R. T. Tiekink, *Z. Kristallogr.-New Cryst. Struct.*, 2003, **218**, 357; (*f*) B.-X. Liu and D.-J. Xu, *Acta Crystallogr., Sect. E: Struct. Rep. Online*, 2005, **61**, m2011; (*g*) X.-L. Niu, J.-M. Dou, C.-W. Hu, D.-C. Li and D.-Q. Wang, *Acta Crystallogr., Sect. E: Struct. Rep. Online*, 2005, **61**, m1909; (*h*) H. Chen, X.-F. Zhang, D.-G. Huang, C.-N. Chen and Q.-T. Liu, *Jiegou Huaxue (Chin. J. Struct. Chem.)*, 2006, **25**, 103; (*i*) G.-D. Sheng, L. Shen, Y.-Z. Jin and J. Mei, *Acta Crystallogr., Sect. E: Struct. Rep. Online*, 2006, **63**, m241; (*j*) C. Zhang and C. Janiak, *Z. Anorg. Allg. Chem.*, 2001, **627**, 1972; (*k*) Z. Zhang, Q.-L. Liu, J.-X. Yang, J.-Y. Wu, Y.-P. Tian, B.-K. Jin, H.-K. Fun, S. Chantrapromma and A. Usman, *Transition Met. Chem.*, 2003, **28**, 930.
9 (*a*) G. Cui, J. Tian and X. Bum, *Nankai Daxue Xuebao, Ziran Kexueban (Chin.) (Acta Scient. Nat. Univ. Nankaiensis)*, 2005, **38**, 32; (*b*) J.-W. Ran, D.-J. Gong and Y.-H. Li, *Acta Crystallogr., Sect. E: Struct. Rep. Online*, 2006, **62**, m3142; (*c*) P.-R. Wei, Q. Li, W.-P. Leung and T. C. W. Mak, *Polyhedron*, 1997, **16**, 897; (*d*) C.-M. Che, W.-T. Tang, K.-Y. Wong, W.-T. Wong and T.-F. Lai, *J. Chem. Res.*, 1991, **30**, 401; (*e*) T. Nagataki, Y. Tachi and S. Itoh, *Chem. Commun.*, 2006, 4016; (*f*) B.-S. Zhang, *Z. Kristallogr.-New Cryst. Struct.*, 2007, **222**, 274; (*g*) X.-L. Niu, J.-M. Dou, C.-W. Hu, D.-C. Li and D.-Q. Wang, *Acta Crystallogr., Sect. E: Struct. Rep. Online*, 2005, **61**, m2538; (*h*) C. J. Shen, J.-S. Chen, T.-L. Sheng, R.-B. Fu, S.-M. Hu, S.-C. Xiang, Z.-T. Qin, X. Wang, Y.-M. He and X.-T. Wu, *Jiegou Huaxue (Chin. J. Struct. Chem.)*, 2008, **27**, 899; (*i*) C.-H. Zhang, S.-P. Tang, M.-S. Chen, D.-Z. Luang and Y.-F. Deng, *Wuji Huaxue Xuebao (Chin.) (Chin. J. Inorg. Chem.)*, 2008, **24**, 1519; (*j*) V. Gómez and M. Corbella, *J. Chem. Cryst.* submitted; (*k*) M. U. Triller, W.-Y. Hsieh, V. L. Pecoraro, A. Rompel and B. Krebs, *Inorg. Chem.*, 2002, **41**, 5544.
10 (*a*) S. Tomida, H. Matsushima, M. Koikawa and T. Tokii, *Chem. Lett.*, 1999, 437; (*b*) H. Oshio, E. Ino, I. Mogi and T. Ito, *Inorg. Chem.*, 1993, **32**, 5697; (*c*) C. Ma, W. Wang, X. Zhang, C. Chen, Q. Liu, H. Zhu, D. Liao and L. Li, *Eur. J. Inorg. Chem.*, 2004, 3522; (*d*) G. Fernandez, M. Corbella, J. Mahia and M. A. Maestro, *Eur. J. Inorg. Chem.*, 2002, 2502; (*e*) B. Albela, M. Corbella, J. Ribas, I. Castro, J. Sletten and H. Stoeckli-Evans, *Inorg. Chem.*, 1998, **37**, 788.
11 (*a*) C. J. Milios, E. Kefalloniti, C. P. Raptopoulou, A. Terzis, A. Escuer, R. Vicente and S. P. Perlepes, *Polyhedron*, 2004, **23**, 83; (*b*) A. Bianchi, L. Calabi, C. Giorgi, P. Losi, P. Mariani, D. Palano, P. Paoli, P. Rossi and B. Valtancoli, *J. Chem. Soc., Dalton Trans.*, 2001, 917; (*c*) Z.-P. Kong, R.-L. Bao, X.-G. Zhou, Z. Pang, L. Jiang, Z.-X. Chen and B. Yue, *Z. Kristallogr.-New Cryst. Struct.*, 2005, **220**, 85; (*d*) F. Nepveu, M. Berkaoui, P. Castan and L. Waiz, *Z. Kristallogr.*, 1994, **209**, 351; (*e*) N. Okabe and N. Oya, *Acta Crystallogr., Sect. C: Cryst. Struct. Commun.*, 2000, **56**, 1416; (*f*) A. M. Baruak, A. Karmakar and J. B. Baruah, *The Open Inorganic Chemistry Journal*, 2008, **2**, 62; (*g*) K. Yamamato, I. Miyahara, A. Ichimura, K. Hirotsu, Y. Kojima, H. Sakurai, D. Shiomi, K. Sato and T. Takui, *Chem. Lett.*, 1999, 295; (*h*) C.-Y. Cheng and S.-L. Wang, *Acta Crystallogr., Sect. C: Cryst. Struct. Commun.*, 1991, **47**, 1734; (*i*) F.-Q. Wang, X.-J. Zheng, Y.-H. Wan, K.-Z. Wang and L.-P. Jin, *Polyhedron*, 2008, **27**, 717; (*j*) C. Policar, S. Durot, F. Lambert, M.

Cesario, F. Ramiandrasoa and I. Morgenstern-Badarau, *Eur. J. Inorg. Chem.*, 2001, 1807.
12 (*a*) D. Moon, J. Kim, M. Oh, B. S. Suh and M. S. Lah, *Polyhedron*, 2008, **27**, 447; (*b*) S. Durot, C. Policar, G. Pelosi, F. Bisceglie, T. Mallah and J.-P. Mahy, *Inorg. Chem.*, 2003, **42**, 8072; (*c*) F. Nepveu, N. Gaultier, N. Korber, J. Jaud and P. Castan, *J. Chem. Soc., Dalton Trans.*, 1995, 4005; (*d*) S. Sen, S. Mitra, D. Luneau, M. S. El Fallah and J. Ribas, *Polyhedron*, 2006, **25**, 2737; (*e*) H. Iikura and N. Nagata, *Inorg. Chem.*, 1998, **37**, 4702; (*f*) J. Kim, J. M. Lim, M. C. Suh and H. Yun, *Polyhedron*, 2001, **20**, 1947; (*g*) C. Baffert, M.-N. Collomb, A. Deronzier, S. Kjaergaard-Knudsen, J.-M. Latour, K. H. Lund, C. J. McKenzie, M. Mortensen, L. P. Nielsen and N. Thorup, *Dalton Trans.*, 2003, 1765; (*h*) C. Jiang, X. Zhu, Z.-P. Yu and Z.-Y. Wang, *Inorg. Chem. Commun.*, 2003, **6**, 706.
13 (*a*) C. H. L. Kennard, G. Smith, E. J. O'Reilly and W. Chiangjin, *Inorg. Chim. Acta*, 1983, **69**, 53; (*b*) E. Garribba, G. Micera and M. Zema, *Inorg. Chim. Acta*, 2004, **357**, 2038; (*c*) T. Glowiak, H. Kozlowski, L. S. Erre and G. Micera, *Inorg. Chim. Acta*, 1995, **236**, 149.
14 (*a*) S. Gao, J.-W. Liu, L.-H. Huo, H. Zhao and J.-G. Zhao, *Acta Crystallogr., Sect. C: Cryst. Struct. Commun.*, 2005, **61**, m25; (*b*) J.-L. Lin and Y.-Q. Zheng, *Acta Crystallogr., Sect. E: Struct. Rep. Online*, 2006, **62**, m3131; (*c*) C.-Y. Sun, S. Gao and L.-P. Jin, *Eur. J. Inorg. Chem.*, 2006, 2411; (*d*) M. J. Plater, M. R. St. J. Foreman, R. A. Howie, J. M. S. Skakle, E. Coronado, C. J. Gomez-Garcia, T. Gelbrich and M. B. Hursthouse, *Inorg. Chim. Acta*, 2001, **319**, 159; (*e*) M. J. Plater, M. R. St. J. Foreman, E. Coronado, C. J. Gomez-Garcia and A. M. Z. Slawin, *J. Chem. Soc., Dalton Trans.*, 1999, 4209.
15 S. Stoll and A. Schweiger, *J. Magn. Reson.*, 2006, **178**, 42.
16 A. Altomare, M. C. Burla, M. Camalli, G. L. Cascarano, C. Giacovazzo, A. Guagliardi, A. G. G. Moliterni, G. Polidori and R. Spagna, *SIR97: A New Tool for Crystal Structure Determination and Refinement; J. Appl. Crystallogr.*, 1999, **32**, 115.
17 G. M. Sheldrick, *SHELXL97: A program for crystal structure refinement*, University of Goettingen, Germany, 1997.
18 G. M. Sheldrick, *SHELXS: A program for automatic solution of crystal structure*, University of Goettingen, Germany, 1997.
19 V. Gómez and M. Corbella, *Eur. J. Inorg. Chem.*, 2009, 4471 and references cited therein.
20 B. Deacon and R. J. Phillips, *Coord. Chem. Rev.*, 1980, **33**, 227.
21 R. L. Rardin, W. B. Tolman and S. J. Lippard, *New J. Chem.*, 1991, **15**, 417.
22 J. H. Van Vleck, *The Theory of Electric and Magnetic Susceptibilities*, Oxford University Press, London, 1932.
23 O. Kahn, *Molecular Magnetism*, Wiley-VCH, New York, 1993.
24 M. Wang, B. Wang and Z. Chen, *J. Mol. Struct.: THEOCHEM*, 2007, **816**, 103.
25 (*a*) A. J. Downard, V. McKee and S. S. Tandon, *Inorg. Chim. Acta*, 1990, **173**, 181; (*b*) S. Koizumi, M. Nihei and H. Oshio, *Chem. Lett.*, 2004, **33**, 896; (*c*) H. Wada, K. Motoda, M. Ohba, H. Sakiyama, N. Matsumoto and H. Okawa, *Bull. Chem. Soc. Jpn.*, 1995, **68**, 1105; (*d*) W.-Y. Hsieh, C. M. Zalenski, V. L. Pecoraro, P. E. Fanwick and S. Liu, *Inorg. Chim. Acta*, 2006, **359**, 228; (*e*) A. Gelasco, M. L. Kirk, J. W. Kampf and V. L. Pecoraro, *Inorg. Chem.*, 1997, **36**, 1829; (*f*) I. A. Koval, M. Huisman, A. F. Stassen, P. Gamez, M. Lutz, A. L. Spek, D. Pursche, B. Krebs and J. Reedijk, *Inorg. Chim. Acta*, 2004, **357**, 294; (*g*) D. J. Hodgson, B. J. Schwartz and T. N. Sorrell, *Inorg. Chem.*, 1989, **28**, 2226; (*h*) C. Hureau, E. Anxolabehere-Mallart, M. Nierlich, F. Gonnet, E. Riviere and G. Blondin, *Eur. J. Inorg. Chem.*, 2002, 2710; (*i*) D. P. Kessissoglou, W. M. Butler and V. L. Pecoraro, *Inorg. Chem.*, 1987, **26**, 495; (*j*) L. Sabater, C. Hureau, G. Blain, R. Guillot, P. Thuery, E. Riviere and A. Aukauloo, *Eur. J. Inorg. Chem.*, 2006, 4324; (*k*) M. Qian, S. Gou, S. Chantrapromma, S. S. S. Raj, H.-K. Fun, Q. Zeng, Z. Yu and X. You, *Inorg. Chim. Acta*, 2000, **305**, 83.
26 (*a*) M. Ryazanov, S. Troyanov, M. Baran, R. Szymczak and N. Kuzmina, *Polyhedron*, 2004, **23**, 879; (*b*) J.-M. Shi, Z. Liu, W.-N. Li, H. Y. Zhao and L.-D. Liu, *J. Coord. Chem.*, 2007, **60**, 1077; (*c*) Z.-H. Jiang, B.-W. Sun, D.-Z. Liao, G.-L. Wang, B. Donnadieu and J.-P. Tuchagues, *Inorg. Chim. Acta*, 1998, **279**, 76; (*d*) M. D. Carducci and R. J. Doedens, *Inorg. Chem.*, 1989, **28**, 2492; (*e*) L.-Y. Wang, X.-Q. Wang, K. Jiang, J.-L. Chang and Y.-F. Wang, *J. Mol. Struct.*, 2007, **840**, 14.
27 D.-K. Cao, J. Xiao, J.-W. Tong, Y.-Z. Li and L.-M. Zheng, *Inorg. Chem.*, 2007, **46**, 428.
28 R. Ruiz-Garcia, E. Pardo, M. C. Muñoz and J. Cano, *Inorg. Chim. Acta*, 2007, **360**, 221.
29 F. Nesse, *J. Am. Chem. Soc.*, 2006, **128**, 10213; S. Zein, C. Duboc, W. Lubitz and F. Nesse, *Inorg. Chem.*, 2008, **47**, 134.